Community size predicts temporal β-diversity at local but not regional scales

Cristina M. Jacobi[1] & Tadeu Siqueira[1,2]

[1] Departamento de Biodiversidade, Instituto de Biociências, Universidade Estadual Paulista (UNESP), Rio Claro, SP, Brasil

[2] School of Biological Sciences, University of Canterbury, Private Bag 4800, Christchurch 8140, New Zealand, ORCID: 0000-0001-5069-290

Corresponding author: Tadeu Siqueira (tadeu.siqueira@unesp.br)

Open research statement: Data are already published and publicly available, with those items properly cited in this submission. Fish data are available through the iDiv Biodiversity Portal: https://doi.org/10.25829/idiv.1873-10-4000. Temperature and precipitation were obtained from TerraClimate (https://www.climatologylab.org/terraclimate.htmlv). Hydrography data are available at HydroRIVERS (https://www.hydrosheds.org/products/hydrorivers) and HydroBasin https://www.hydrosheds.org/products/hydrobasins.

Keywords: demographic stochasticity, ecological drift, community size, compositional variability, spatial scale, spatial synchrony, metacommunities

Abstract

Understanding what drives temporal changes in community composition is urgent given widespread population declines that increase vulnerability to demographic noise. We investigated how demographic stochasticity and environmental variability relate to compositional variability both locally (temporal β-diversity) and regionally (temporal changes in spatial β-diversity). To do this, we first simulated communities without environmental selection to test whether commonly used β-diversity metrics were robust to demographic stochasticity alone. In the absence of environmental forcing, a rank-change metric showed no consistent relationship with community size, confirming that observed size effects in empirical data would not be artifacts of the metric. We then analyzed 468 riverine fish community time series collected between 1981 and 2019 across 39 regions spanning three biogeographic realms, modeling local and regional compositional variability against community size, its temporal variability, species richness, rarity, and environmental variation and synchrony. Empirical analyses revealed scale dependence in the processes shaping compositional change. At the local scale, internal community properties were more important. Smaller median community size and greater fluctuations in total abundance were related to higher temporal β-diversity, consistent with a stronger role of demographic stochasticity in small communities. Higher species richness also increased temporal β-diversity, likely by enlarging the pool of possible colonists and increasing the number of feasible community states. At the regional scale, however, these factors had little influence. Instead, the spatial synchrony of precipitation emerged as the main predictor of temporal changes in spatial β-diversity. Metacommunities embedded in more synchronized environments exhibited less temporal variability in among-site dissimilarity, suggesting that synchronized environmental forcing constrains spatial reshuffling of communities over time. Together, these results reveal a scale-dependent shift in the processes influencing

compositional variability. Local temporal β-diversity can be primarily driven by demographic stochasticity and richness effects, whereas regional compositional dynamics by environmental factors. This integration of demographic and environmental perspectives highlights how the balance between internal and external processes shifts across scales. It is important to understand how such processes interact in a time when biodiversity is declining, populations are getting smaller and climates are becoming more variable. These trends could change how ecological communities vary over time.

Introduction

Ecosystems show decreasing temporal variability when analyzed across broader spatial scales, higher organizational levels, or more complex trophic structures (Wang et al. 2019, Kéfi et al. 2019, Hammond et al. 2020, Siqueira et al. 2024). This scaling pattern has been associated to multiple mechanisms, mainly deterministic ones such as compensatory species dynamics (Gonzalez and Loreau 2009), mobile predators (McCann et al. 2005) and spatially synchronized environmental effects (Steiner et al. 2013), as well as statistical averaging (Doak et al. 1998). Stochastic processes, particularly demographic stochasticity, are also expected to influence variability, especially where local population sizes are small (Lande et al. 2003). Yet we lack a clear understanding of how random demographic events at the individual and population level cascade into turnover in species composition through time, and how those effects aggregate across local communities to alter metacommunity temporal dynamics. This gap persists despite the growing recognition of stochastic processes in ecosystems (Vellend 2016, Leibold and Chase 2018) and the increasing need of understanding biodiversity temporal dynamics under global change (Shimadzu et al. 2015, Magurran et al. 2019, Tatsumi et al. 2021, Dornelas et al. 2023).

Demographic stochasticity is chance variation in individual fates (births, deaths) whose relative influence increases as population size declines (Reed and Hobbs 2004, Melbourne and Hastings 2008). At the population level, these random events produce drift-like temporal trajectories (Lande 1993). When such dynamics occurs independently among localities it generates asynchronous population dynamics that, when scaled up, can result in large within-site compositional turnover through time (high temporal β-diversity) and also in high among-site dissimilarity in snapshot surveys (Siqueira et al. 2020). Thus, spatial patterns observed at a single time may reflect underlying stochastic dynamics operating asynchronously across sites.

Environmental stochasticity (i.e., temporal variation in abiotic or biotic conditions) differs qualitatively from demographic noise because it can affect many individuals simultaneously (Lande et al. 2003). These processes leave different empirical signatures. Whereas demographic stochasticity generates uncorrelated, site-specific random walks in abundance (Melbourne and Hastings 2008), environmental stochasticity can produce synchronized temporal responses across sites if the driver is spatially correlated (Bjørnstad et al. 1999). The relative importance of each stochasticity type depends on the magnitude, temporal pattern, and spatial correlation of environmental variation relative to population size. So, accounting for spatial scale and correlation structure is central to interpreting both static and temporal diversity patterns.

These contrasting dynamics map directly onto temporal changes in spatial β-diversity (Tatsumi et al. 2021). Asynchronous, drift-like turnover can maintain or amplify spatial β-diversity over time, whereas synchronized environmental factors tends to homogenize communities across sites. Both processes can also increase local extinction risk when populations are small (Lande et al. 2003), and the spatial pattern of extinctions determines whether communities differentiate or homogenize through time (Olden et al. 2004). The balance between drift, environmental selection, and dispersal ultimately determines how local population fluctuations scale up to regional compositional change, even though dispersal and spatial averaging may mitigate these effects (Arim et al. 2023, Suzuki and Economo 2024).

Disentangling these mechanisms in observational data is difficult because unmeasured or noisy environmental drivers can mimic demographic signals. Empirical studies therefore rely on indirect tests and complementary diagnostics: using community size (e.g., total number of individuals; Orrock & Watling, 2010) or area (Liu et al. 2018) as proxies for susceptibility to demographic noise, checking variance–mean relationships and temporal metrics, comparing observed patterns to null simulations, and applying dynamic models that

partition demographic and environmental stochasticity (Cohen et al. 2013, Nakadai 2021, Knape et al. 2023). For example, if smaller communities exhibit higher compositional variability or weaker environmental relationships, this suggests demographic noise plays a role (Gilbert and Levine 2017, Siqueira et al. 2020). Recent research supported this strategy by showing that while the strength of environmental filtering increased with community size, spatial β-diversity in fish communities decreased (Jacobi and Siqueira 2023). It is important to note, however, that this approach employs size–diversity relationships to assess the relative contributions of environmental and demographic processes rather than treating community or ecosystem size as a direct indicator of stochasticity.

Considering this framing and the widespread population declines that potentially increase vulnerability to demographic noise (McCallum 2015, He et al. 2019, Almond et al. 2020), we investigated how demographic stochasticity and environmental variability relate to compositional variability both locally (temporal β-diversity) and regionally (temporal changes in spatial β-diversity). If compositional variability is mostly driven by demographic stochasticity, then (1) abundance-based temporal β-diversity should increase as mean community size decreases, and (2) there should be weak statistical relationship between compositional changes and measuared environmental factors.

To test these expectations, we first used simulations to validate whether β-diversity metrics reliably captured demographic variability. We then analyzed 468 fish-community time series (1981–2019; 39 regions), modeling local and regional compositional variability against community size, environmental drivers, and species richness. By combining simulation and empirical approaches, we are able to measure the contributions of environmental processes and demographic drift to changes in the temporal composition of communities of different sizes.

Material and methods

Data

We ran our empirical analyses using data from two databases. From the RivFishTIME (Comte et al. 2021), we obtained time series count data of riverine fish around the globe. TerraClimate (Abatzoglou et al. 2018) provided high-resolution monthly data for environmental variables, from which we calculated annual averages for precipitation, maximum air temperature, and minimum air temperature (which is a good proxy for water temperature (Stefan and Preud'homme 1993).

We defined a metacommunity as the set of sites within basin delineations (HydroBASINS level 7) (Lehner and Grill 2013) and assigned a Strahler stream order for each sampled site using information from the HydroRIVERS network (Lehner and Grill 2013). We then selected metacommunities that met the following criteria: (1) comprised at least five communities in first to third-order streams, (2) were sampled at least four times in different years, and (3) had at least five species. When dealing with metacommunity data comprising multiple sampling events per year, we selected the sampling date with the highest number of sampled sites to maximize the sample size. These steps resulted in 468 communities distributed within 39 metacommunities, sampled from 1981 to 2019, located in the Australasia (12), Nearctic (12), and Palearctic (15) biogeographical realms (see Appendix S1: Figure S1). These metacommunities were composed on average of 12 communities (standard deviation = 9) sampled, on average, 11 times in the time-series (standard deviation = 5) with an average temporal extent of 14 years (standard deviation = 5). All data selection and manipulation were performed in R v. 4.2.1 (www.r-project.org) using the packages ncdf4 (Pierce 2023), mapview (Appelhans et al. 2023) raster (Hijmans et al. 2023), sf (Pebesma 2018, Pebesma and Bivand 2023), sp (Pebesma and Bivand 2005, Bivand et al. 2013), and tidyverse (Wickham et al. 2019).

156

157 **Metrics of community size and species richness**

158 We quantified local community size as the median number of individuals over time,
159 representing the central tendency of population vulnerability to demographic stochasticity;
160 that is, smaller values indicated communities where demographic stochasticity was more
161 likely to occur. At the regional scale, we calculated metacommunity size as the median of
162 these local medians over time. In addition to these measures of central tendency, we also
163 included the temporal coefficient of variation (CV) in community size as a predictor of
164 compositional variability at both local and regional scales.

165 Additionally, we calculated the proportion of species in the lowest abundance
166 category (PL), which represents the share of relatively rare species in the regional species
167 pool, following (Xiao et al. 2025). For each site we defined PL as the proportion of species
168 whose mean abundance over the time series (for that specific site) fell in the lowest
169 abundance bin of the observed species–abundance distribution, and we computed an
170 analogous PL for each region. PL at the local scale was calculated by considering the whole
171 set of samples within a community through time (the whole time series for each community)
172 as the species pool. For regional PL, we calculated PL at the metacommunity level (the whole
173 metacommunity was the species pool) for each time step and then used the median of these
174 values for each metacommunity. For our regional models, we also included the temporal
175 coefficient of variation (CV) of PL to account for fluctuations in the relative share of rare
176 species through time. We included PL as an additional predictor at both local and regional
177 scales because the share of relatively rare species may modulate susceptibility to
178 demographic drift and to environment-driven losses, and thus influence temporal β-diversity.

179 To represent local species richness, we estimated the median asymptotic richness of
180 each community over time. At the regional scale, we estimated gamma diversity as the

median asymptotic richness of each metacommunity over time. Asymptotic richness was estimated with the iNEXT package (Hsieh et al. 2022), which combines extrapolation and interpolation techniques.

Environmental predictors of temporal variability in species composition

Environmental predictors of temporal variability in species composition included the coefficient of variation (CV) of maximum (CV tmax) and minimum (CV tmin) temperature and of precipitation (CV ppt). These metrics were measured by dividing the standard deviation of temperature and precipitation values at each site over time by the mean of these values.

We measured environmental synchrony within metacommunities by calculating the correlation of each environmental variable between communities over time (synchrony of maximum temperature = syn tmax, synchrony of minimum temperature = syn tmin, synchrony of precipitation = syn ppt). A high correlation or environmental synchrony would indicate that the environmental conditions being analyzed changed similarly across sites, while a low synchrony indicates that environmental conditions vary more independently across sites.

Finally, we also investigated if sample size (number of samples collected) and time series length (temporal extent of sampling) at both community and metacommunity levels, and metacommunity spatial extent could counfound the estimated relationships. We measured the spatial extent of each metacommunity by calculating the mean Euclidean distance between the central point of each metacommunity and its constituent communities. The mean distance between communities provides a measure of the overall spatial extent of the region encompassed by the metacommunity. We used the geosphere package (Hijmans 2022) to perform these calculations.

206

207 **Metrics of temporal variability in species composition**

208 A major challenge involved in relating community size to metrics of spatial and
209 temporal variability in species composition is that they can be mathematically related to each
210 other regardless of the underlying assembly process (Beck et al. 2013, Chase and Knight
211 2013, Barwell et al. 2015, Cao et al. 2021). Thus, to select appropriate metrics of temporal
212 variability that could be modeled against community size, we first simulated
213 metacommunities without environmental selection, i.e. under purely neutral-like dynamics,
214 according to the following steps.

215 Riverine networks were simulated using the mcbrnet R package (Terui and Pomeranz
216 2023). We first simulated random branching networks using the function brnet, which were
217 then used in the mcsim function to simulate metacommunity dynamics. Since we were
218 interested in simulating metacommunities without niche differentiation, we simulated species
219 with similar niches along a spatially homogeneous environment. Carrying capacity was
220 similar within communities in a given metacommunity but varied randomly among
221 metacommunities (ranging from 50 to 150 individuals). We manipulated random mortality
222 intensity and carrying capacity to approximate metacommunity sizes observed in the
223 empirical datasets. We assigned the same dispersal probability to all species in each
224 simulation but conducted multiple simulations with different probabilities (high: 1,
225 intermediate: 0.5, low: 0.1) to assess their impact on the relationship between a metric of
226 temporal variability and community size.

227 Each simulation included 39 metacommunities, matching the empirical dataset. These
228 metacommunities contained 5 to 30 communities and 5 to 48 species, reflecting the observed
229 numbers in the empirical data. We ran each simulation for a total of 1000 time steps. After
230 that, we selected species composition in ten time-steps (100, 200, 300, 400, 500, 600, 700,

800, 900, and 1000) as our temporal samples to measure the temporal variability at both local (within each community) and regional (among communities) scales using different metrics: (i) temporal variability in species composition at the local and regional scales, employing the metric proposed by Lamy *et al.*, (2021) and implemented in the ltmc package (Sokol and Lamy 2022) and (ii) temporal beta diversity, measured as the median of species rank changes (Avolio et al. 2019) within each community over time, using the RAC_change function in the codyn package (Hallett et al. 2020), and (iii) temporal variation in spatial turnover within metacommunities, via the RAC_difference function in the codyn package (Hallett et al. 2020). The median difference in species rank among communities within metacommunities was calculated at each time step.

Finally, we regressed all these metrics of temporal variability against median community size over time and compared the outcomes. Because the assembly of our simulated metacommunities excluded environmental selection, any size effect would indicate that the metric was biased by sampling or other artifacts rather than reflecting true demographic stochasticity. Thus, a lack of relationship between community size and temporal variability in these neutral simulations provides a necessary baseline for evaluating which metrics can be reliably interpreted in the empirical analyses.

Linear models

Modelling temporal β-diversity

The response variable selected to represent temporal variability in species composition, rank change (see results), represents proportional values bounded between 0 and 1. To meet model assumptions of homoscedasticity and normality of residuals for Gaussian models, rank change was transformed using a logit transformation with a small offset (1e-6) to avoid zeros. Predictor variables were standardized (mean = 0, SD = 1) to

improve model convergence and facilitate interpretation of effect sizes. We assessed multicollinearity among all predictors using variance inflation factors (VIF), and all values were below 2, indicating no cause for concern. We also tested for and found no significant correlation between rank change and two potential confounding variables, time series length and number of samples per time point. As we had no a priori hypotheses for these variables, they were excluded from the final models to aid interpretation and avoid overfitting.

We evaluated a series of increasingly complex linear models to explain temporal variability in local species composition (logit–transformed rank change). First, we fitted a beta regression including our standardized predictors: median community size, its temporal coefficient of variation (CV), the proportion of species in the lowest abundance category (PL), estimated richness, and the CV of minimum temperature, maximum temperature, and precipitation. Next, we added a random intercept for metacommunity identity to account for non-independence among sites, and then introduced a dispersion submodel so that residual variance could vary as a function of community size, CV of community size, and PL. Likelihood-ratio tests and AIC comparisons showed that both the random effect and the heteroskedasticity component improved model fit (Appendix S1: Table S1).

Because our response is bounded between 0 and 1, we then refitted this full structure under both beta and Gaussian families. Although AIC favored the beta formulation, graphical and statistical diagnostics of residuals from the beta model (using DHARMa simulated-residual tests) revealed major issues with dispersion and quantile deviations. In contrast, the same diagnostics showed that the Gaussian location–scale model more closely met underlying assumptions, with a uniform QQ-plot and no dispersion issues. Furthermore, a check for out-of-bounds predictions from the Gaussian model found that none of the predictions fell outside the [0,1] interval. Based on these checks, we selected the Gaussian location–scale model for all subsequent inference. We estimated model explanatory power

using marginal and conditional R^2 values derived from the location component of the Gaussian GLMM, which included fixed effects and a random intercept for metacommunity identity. These R^2 values quantify the proportion of variance explained by the fixed effects alone (marginal R^2) and by both fixed and random effects combined (conditional R^2), but do not account for variation explained by the dispersion (variance) model.

Modelling temporal changes in spatial β-diversity

To analyze temporal changes in spatial β-diversity, we followed a similar model-building and selection procedure as we did for temporal β-diversity. The response variable, the coefficient of variation in species ranks across sites within a metacommunity (CV_rank), is also a proportional measure bounded between 0 and 1. Consequently, it was logit-transformed with a small offset (1e-6) to avoid zeros, and all predictor variables were standardized (mean = 0, SD = 1). We again tested for correlations with time series length and number of samples per time point. Because we found none, we excluded these variables from subsequent models as they were not part of our core hypotheses.

We then assessed multicollinearity among our candidate predictors. Variance inflation factors (VIF) identified high collinearity among the temperature and precipitation synchrony metrics. We retained only synchrony in precipitation, which is most biologically relevant for our study systems, resulting in all VIF values below acceptable thresholds.

We then evaluated a series of models. First, we fitted a beta regression with a logit link including all standardized predictors. Unlike the model for temporal β-diversity, the addition of a dispersion submodel (allowing residual variance to vary as a function of metacommunity community size, median proportion of rare species, synchrony in precipitation, and regional CV of community size) did not improve model fit (LRT: $\chi^2 = 7.94$, df = 4, p = 0.094). We therefore proceeded with the simpler homoscedastic beta regression.

We compared this beta GLM to a Gaussian GLM with an identity link. In contrast to our model for temporal β-diversity, AIC favored the beta model (ΔAIC = 10.2; Appendix S1). Diagnostic checks using DHARMa revealed no issues with dispersion, uniformity, or outliers for the beta model, confirming that it met all necessary assumptions. A check for out-of-bounds predictions confirmed that none of the predictions fell outside the [0,1] interval. Based on these results, we selected the homoscedastic beta regression for all subsequent inference. A full summary of the model selection procedure, including AIC values for all compared models, is provided in Appendix S1: Table S1.

All model fitting was conducted in glmmTMB (Brooks et al. 2017), residuals were checked with DHARMa (Hartig 2024), and p-values for fixed effects were obtained from Type II Wald χ^2 tests in the car package (Fox and Weisberg 2019). All analyses were conducted in R version 4.2.1 (R Core Team, 2022).

Results

Metrics of temporal variability in simulated metacommunities

Our simulations indicated that most metrics of temporal variability in species composition had a relationship with community size. The LTMC metric (temporal turnover within communities) exhibited a consistent negative relationship with community size at the local scale and, at the regional scale, showed a negative relationship in some simulations, whereas in others no such pattern was observed (see Appendix S1: Table S2). However, when a relationship was present at the regional scale, it exhibited high explanatory power. The species rank difference metric was positively related to community size in most simulations at the regional scale; however, the explanatory power of the models (R^2) was consistently low across all simulation scenarios (mean $R^2 = 0.03$; see Appendix S1: Table S2). The species rank change metric (temporal variability in rank abundance curves) was the

only metric that was consistently not related to community size at the local scale (see Appendix S1: Table S2).

Thus, considering that the metrics based on rank-abundance changes showed no spurious relationship with community size under neutral-like dynamics, we used them to analyze the empirical data. More specifically, to represent temporal variability in species composition for each community (temporal β-diversity within communities), we used the species-rank change metric. To represent temporal changes in spatial β-diversity within metacommunities, we used the coefficient of variation of rank differences across years.

Relationships in the empirical dataset

Temporal β-diversity

The final Gaussian location-scale mixed model (family: Gaussian, link: identity) explained a major portion of the variance in temporal β-diversity. The conditional R^2, representing variance explained by both fixed and random effects, was 0.547. The marginal R^2, representing variance explained by fixed effects alone, was 0.191. Temporal β-diversity was primarily influenced by community properties (Table 1).

In the conditional (mean) component of the model, median community size was negatively related to compositional variability ($\beta = -0.006$, SE = 0.002; Wald $\chi^2 = 9.29$, df = 1, $p = 0.0023$; Figure 1a), while temporal variability in community size (CV) was positively related ($\beta = 0.013$, SE = 0.002; Wald $\chi^2 = 28.95$, df = 1, p = 7.44e-08; Figure 1b). Local species richness was also positively related to temporal β-diversity ($\beta = 0.017$, SE = 0.003; Wald $\chi^2 = 26.96$, df = 1, p = 2.08e-07; Figure 1c). The proportion of species in the lowest abundance category (PL) was not a main predictor of temporal β-diversity. Among the climatic predictors, only the coefficient of variation in precipitation showed a marginal

positive relationship; variability in minimum and maximum temperature had no detectable effects (Table 1).

The dispersion component of the model revealed that residual variance declined with increasing community size (β = -0.333, SE = 0.040; z = -8.27, p = 2e-16), temporal variability in community size (β = -0.115, SE = 0.035; z = -3.25, p = 0.00117), and the proportion of species in the lowest abundance category (β = -0.167, SE = 0.032; z = -5.29, p = 1.19e-07; Appendix S1: Table S3).

Temporal changes in spatial β-diversity

The beta regression model (family: beta, link: logit) explained 31% of the variance in temporal variability of spatial β-diversity (Ferrari's R^2 = 0.311). Variability was primarily influenced by environmental synchrony and only marginally by community properties (Table 2). Spatial synchrony in precipitation was negatively related to variability in spatial β-diversity (β = -0.153, SE = 0.073; Wald χ^2 = 4.42, df = 1, p = 0.036), indicating that metacommunities in regions with more synchronized precipitation conditions across sites exhibited more stable spatial structure over time.

The coefficient of variation in community size showed a positive, marginal relationship with temporal variability in spatial β-diversity (β = 0.138, SE = 0.076; Wald χ^2 = 3.29, df = 1, p = 0.069). Community size, gamma diversity, the proportion of rare species, its variability, and mean distance among sites had no effect on temporal variability in spatial β-diversity (Table 2).

Discussion

Our research reveals a scale-dependent shift in the drivers of temporal β-diversity across spatial scales. At the local scale, internal community properties were more important.

Communities with smaller populations exhibited higher temporal compositional variability, whereas those with greater fluctuations in total abundance or higher species richness showed greater temporal β-diversity. In contrast, at the regional scale, an external environmental driver was most influential. Metacommunity-scale compositional variability was primarily determined by the spatial synchrony of precipitation, with more synchronized environments exhibiting less temporal variability in spatial β-diversity. Together, these findings suggest that the mechanisms underpinning temporal compositional dynamics might shift from internal demographic processes to external environmental forcing as observation scale increases.

Our finding that temporal β-diversity is higher in small and variable (in size) communities highlights how the effects of demographic stochasticity can scale up to make community dynamics less predictable. When mean abundance is low, each birth or death event represents a larger proportional change in population size, amplifying random fluctuations and increasing the probability of local extinction (Lande, 1993). On top of this, there sporadic bottlenecks might occur due to high community size variance, when demographic stochasticity is particularly strong, which can reduce or eliminate deterministic fitness differences. Under such conditions, subordinate species can temporarily rise in relative abundance, reshuffling ranks (Orrock and Watling 2010, Gilbert and Levine 2017, Legault et al. 2019) and enabling stochastic reassembly (Leibold and Chase 2018). Additionally, extinction-recolonization dynamics can be exacerbated by community size variability, which further leads to higher, less predictable temporal β-diversity (Tatsumi et al. 2021). The dispersion component of our model reinforces this interpretation, as residual variance declined with increasing mean community size and, to a lesser extent, with its CV, consistent with the scaling of demographic stochasticity.

Beyond community size, other processes can influence the temporal turnover of local communities (Magurran et al. 2019, Saito et al. 2021, Heino et al. 2024). Among the climatic variables tested, interannual variability in precipitation showed a marginal, positive relationship with compositional change ($p = 0.072$), suggestive that this pattern may reflect species differing in their responses to environmental fluctuations (Gonzalez and Descamps-Julien 2004), whereas temperature variability had no detectable effect. Importantly, species richness was positively correlated with temporal β-diversity, probably because more diverse communities include a greater range of demographic and functional responses to stochasticity (Arim et al. 2023). Specifically, greater species richness (over time) increases the number of community states and the probability of turnover through stochastic reassembly by offering a wider pool of possible colonists and alternative trait combinations (Leibold and Chase 2018, Saito et al. 2021). Because the rank_change metric we used standardizes rank shifts across the full species pool (Hallett et al. 2016), our results are unlikely to reflect simple sampling effects, instead pointing to greater inherent dynamism in species-rich systems.

The negative relationship we found between precipitation synchrony and temporal variability in spatial β-diversity is consistent with a Moran-type effect (Ranta et al. 1997, Liebhold et al. 2004). Spatial synchrony means that species abundances at different sites fluctuate together (positive cross-site correlations). If most species change in the same direction and by similar relative amounts across sites, the between-site differences in species composition are maintained through time (sites shift together), so spatial β-diversity remains relatively constant. Similar logic underlies synchrony observed in population dynamics (Liebhold et al. 2004, Koenig and Liebhold 2016) and community-level responses (Gouhier et al. 2010). In contrast, community size did not explain temporal variability in spatial β-diversity, suggesting that demographic stochasticity plays a minor role at this scale. Likewise, while we tested the effect of PL (proportion of rare species) and its temporal CV, their

influence was neglegible compared with precipitation synchrony. Taken together, these results highlight precipitation synchrony as a driver of temporal variability in spatial β-diversity in our systems, while other potential demographic mechanisms appear comparatively weaker.

These interpretations are subject to a few caveats. First, community size is an indirect proxy for demographic susceptibility and does not measure per-capita demographic variance directly. Second, fish counts may be affected by imperfect detection that varies with abundance or habitat. Third, our environmental predictors are annual summaries (TerraClimate) and may miss ecologically important extremes or intra-annual hydrological dynamics (e.g., floods, droughts) that drive turnover in riverine systems.

Understanding these scale-dependent processes is essential in a time of widespread population declines (McCallum 2015, Leuenberger et al. 2025). Population dynamics is fundamentally influenced by demographic stochasticity (Otto and Whitlock 1997, Whitlock 2004, Willi et al. 2006), and our results show that this influence scales up to shape the temporal dynamics of communities. Across spatial scales, we demonstrate a shift in dominance from internal demographic processes to an external environmental factor. This finding combines previously lines of evidence and theory that were either centered on population-level variability or community-level dynamics (Lande 1993, Vindenes and Engen 2017, Jacobi and Siqueira 2023). Ultimately, testing the causal relationships identified here will require new approaches that move beyond correlational analyses to directly quantify and manipulate the underlying processes.

Acknowledgments

We thank Holly Harris and anonymous reviewers for commenting on previous versions of this manuscript. We thank the Coordenação de Aperfeiçoamento de Pessoal de Nível Superior

- Brasil (CAPES) - Funding Code 001 for providing a PhD scholarship to CMJ. TS is supported by funding from the Centre for Research on Biodiversity Dynamics and Climate Change (FAPESP #2021/10639-5) and by a Productivity Grant (Conselho Nacional de Desenvolvimento Científico e Tecnológico, CNPq # 301319/2025-1).

Conflict of Interest Statement: The authors declare no conflict of interest.

461 **References**

462 Abatzoglou, J. T., S. Z. Dobrowski, S. A. Parks, and K. C. Hegewisch. 2018. TerraClimate, a
463 high-resolution global dataset of monthly climate and climatic water balance from
464 1958–2015. Scientific Data 5:170191.
465 Almond, R. E. A., M. Grooten, and T. Petersen. 2020. Bending the curve of biodiversity loss.
466 WWF, Gland.
467 Appelhans, T., F. Detsch, C. Reudenbach, S. Woellauer, S. Forteva, T. Nauss, E. Pebesma, K.
468 Russell, M. Sumner, J. Darley, P. Roudier, P. Schratz, E. I. Marburg, and L. Busetto.
469 2023, October 13. mapview: Interactive Viewing of Spatial Data in R.
470 Arim, M., V. Pinelli, L. Rodríguez-Tricot, E. Ortiz, M. Illarze, C. Fagúndez-Pachón, and A. I.
471 Borthagaray. 2023. Chance and necessity in the assembly of plant communities:
472 Stochasticity increases with size, isolation and diversity of temporary ponds. Journal
473 of Ecology 111:1641–1655.
474 Avolio, M. L., I. T. Carroll, S. L. Collins, G. R. Houseman, L. M. Hallett, F. Isbell, S. E.
475 Koerner, K. J. Komatsu, M. D. Smith, and K. R. Wilcox. 2019. A comprehensive
476 approach to analyzing community dynamics using rank abundance curves. Ecosphere
477 10:e02881.
478 Barwell, L. J., N. J. B. Isaac, and W. E. Kunin. 2015. Measuring β-diversity with species
479 abundance data. The Journal of Animal Ecology 84:1112–1122.
480 Beck, J., J. D. Holloway, and W. Schwanghart. 2013. Undersampling and the measurement of
481 beta diversity. Methods in Ecology and Evolution 4:370–382.
482 Bivand, R., E. Pebesma, and V. Gomez-Rubio. 2013. Applied spatial data analysis with R,
483 Second edition.

484 Bjørnstad, O. N., R. A. Ims, and X. Lambin. 1999. Spatial population dynamics: analyzing
485 patterns and processes of population synchrony. Trends in Ecology & Evolution
486 14:427–432.
487 Brooks, M. E., K. Kristensen, K. J. van Benthem, A. Magnusson, C. W. Berg, A. Nielsen, H.
488 J. Skaug, M. Mächler, and B. M. Bolker. 2017. glmmTMB Balances Speed and
489 Flexibility Among Packages for Zero-inflated Generalized Linear Mixed Modeling.
490 The R Journal 9:378–400.
491 Cao, K., J.-C. Svenning, C. Yan, J. Zhang, X. Mi, and K. Ma. 2021. Undersampling
492 correction methods to control γ-dependence for comparing β-diversity between
493 regions. Ecology 102:e03448.
494 Chase, J. M., and T. M. Knight. 2013. Scale-dependent effect sizes of ecological drivers on
495 biodiversity: why standardised sampling is not enough. Ecology Letters 16:17–26.
496 Cohen, J. E., M. Xu, and W. S. F. Schuster. 2013. Stochastic multiplicative population growth
497 predicts and interprets Taylor's power law of fluctuation scaling. Proceedings of the
498 Royal Society B: Biological Sciences 280:20122955.
499 Comte, L., J. Carvajal-Quintero, P. A. Tedesco, X. Giam, U. Brose, T. Erős, A. F. Filipe, M.
500 Fortin, K. Irving, C. Jacquet, S. Larsen, S. Sharma, A. Ruhi, F. G. Becker, L. Casatti,
501 G. Castaldelli, R. B. Dala-Corte, S. R. Davenport, N. R. Franssen, E. García-Berthou,
502 A. Gavioli, K. B. Gido, L. Jimenez-Segura, R. P. Leitão, B. McLarney, J. Meador, M.
503 Milardi, D. B. Moffatt, T. V. T. Occhi, P. S. Pompeu, D. L. Propst, M. Pyron, G. N.
504 Salvador, J. A. Stefferud, T. Sutela, C. Taylor, A. Terui, H. Urabe, T. Vehanen, J. R. S.
505 Vitule, J. O. Zeni, and J. D. Olden. 2021. RivFishTIME: A global database of fish
506 time-series to study global change ecology in riverine systems. Global Ecology and
507 Biogeography 30:38–50.

508 Doak, D. F., D. Bigger, E. K. Harding, M. A. Marvier, R. E. O'Malley, and D. Thomson.
509 1998. The Statistical Inevitability of Stability-Diversity Relationships in Community
510 Ecology. The American Naturalist 151:264–276.
511 Dornelas, M., J. M. Chase, N. J. Gotelli, A. E. Magurran, B. J. McGill, L. H. Antão, S. A.
512 Blowes, G. N. Daskalova, B. Leung, I. S. Martins, F. Moyes, I. H. Myers-Smith, C. D.
513 Thomas, and M. Vellend. 2023. Looking back on biodiversity change: lessons for the
514 road ahead. Philosophical Transactions of the Royal Society B: Biological Sciences
515 378:20220199.
516 Fox, J., and S. Weisberg. 2019. An {R} Companion to Applied Regression, Third Edition.
517 Thousand Oaks CA: Sage.
518 Gilbert, B., and J. M. Levine. 2017. Ecological drift and the distribution of species diversity.
519 Proceedings of the Royal Society B: Biological Sciences 284:20170507.
520 Gonzalez, A., and B. Descamps-Julien. 2004. Population and community variability in
521 randomly fluctuating environments. Oikos 106:105–116.
522 Gonzalez, A., and M. Loreau. 2009. The Causes and Consequences of Compensatory
523 Dynamics in Ecological Communities. Annual Review of Ecology, Evolution, and
524 Systematics 40:393–414.
525 Gouhier, T. C., F. Guichard, and A. Gonzalez. 2010. Synchrony and Stability of Food Webs in
526 Metacommunities. The American Naturalist 175:E16–E34.
527 Hallett, L., M. Avolio, I. Carroll, S. Jones, A. MacDonald, D. Flynn, P. Slaughter, J.
528 Ripplinger, S. Collins, C. Gries, and M. Jones. 2020. .
529 Hallett, L. M., S. K. Jones, A. A. M. MacDonald, M. B. Jones, D. F. B. Flynn, J. Ripplinger,
530 P. Slaughter, C. Gries, and S. L. Collins. 2016. CODYN: An R package of community
531 dynamics metrics. Methods in Ecology and Evolution 7:1146–1151.

Hammond, M., M. Loreau, C. de Mazancourt, and J. Kolasa. 2020. Disentangling local, metapopulation, and cross-community sources of stabilization and asynchrony in metacommunities. Ecosphere 11:e03078.

Hartig, F. 2024. DHARMa: Residual Diagnostics for Hierarchical (Multi-Level / Mixed) Regression Models.

He, F., C. Zarfl, V. Bremerich, J. N. W. David, Z. Hogan, G. Kalinkat, K. Tockner, and S. C. Jähnig. 2019. The global decline of freshwater megafauna. Global Change Biology 25:3883–3892.

Heino, J., L. M. Bini, J. García-Girón, F. M. Lansac-Tôha, M. Lindholm, and R. J. Rolls. 2024. Navigating the spatial and temporal aspects of beta diversity to facilitate understanding biodiversity change. Global Ecology and Conservation 56:e03343.

Hijmans, R. 2022. _geosphere: spherical trigonometry_.

Hijmans, R. J., J. van Etten, M. Sumner, J. Cheng, D. Baston, A. Bevan, R. Bivand, L. Busetto, M. Canty, B. Fasoli, D. Forrest, A. Ghosh, D. Golicher, J. Gray, J. A. Greenberg, P. Hiemstra, K. Hingee, A. Ilich, I. for M. A. Geosciences, C. Karney, M. Mattiuzzi, S. Mosher, B. Naimi, J. Nowosad, E. Pebesma, O. P. Lamigueiro, E. B. Racine, B. Rowlingson, A. Shortridge, B. Venables, and R. Wueest. 2023, October 14. raster: Geographic Data Analysis and Modeling.

Hsieh, T., K. Ma, and A. Chao. 2022. iNEXT: iNterpolation and EXTrapolation for species diversity.

Jacobi, C. M., and T. Siqueira. 2023. High compositional dissimilarity among small communities is decoupled from environmental variation. Oikos 2023:e09802.

Kéfi, S., V. Domínguez-García, I. Donohue, C. Fontaine, E. Thébault, and V. Dakos. 2019. Advancing our understanding of ecological stability. Ecology Letters 22:1349–1356.

Knape, J., M. Paquet, D. Arlt, I. Kačergytė, and T. Pärt. 2023. Partitioning variance in population growth for models with environmental and demographic stochasticity. Journal of Animal Ecology 92:1979–1991.

Koenig, W. D., and A. M. Liebhold. 2016. Temporally increasing spatial synchrony of North American temperature and bird populations. Nature Climate Change 6:614–617.

Lamy, T., N. I. Wisnoski, R. Andrade, M. C. N. Castorani, A. Compagnoni, N. Lany, L. Marazzi, S. Record, C. M. Swan, J. D. Tonkin, N. Voelker, S. Wang, P. L. Zarnetske, and E. R. Sokol. 2021. The dual nature of metacommunity variability. Oikos 130:2078–2092.

Lande, R. 1993. Risks of Population Extinction from Demographic and Environmental Stochasticity and Random Catastrophes. The American Naturalist 142:911–927.

Lande, R., S. Engen, and B.-E. Sæther. 2003. Stochastic Population Dynamics in Ecology and Conservation. Oxford University Press.

Legault, G., J. W. Fox, and B. A. Melbourne. 2019. Demographic stochasticity alters expected outcomes in experimental and simulated non-neutral communities. Oikos 128:1704–1715.

Lehner, B., and G. Grill. 2013. Global river hydrography and network routing: baseline data and new approaches to study the world's large river systems. Hydrological Processes 27:2171–2186.

Leibold, M. A., and J. M. Chase. 2018. Metacommunity Ecology, Volume 59. Princeton University Press, Princeton, NJ.

Leuenberger, W., J. W. Doser, M. W. Belitz, L. Ries, N. M. Haddad, W. E. Thogmartin, and E. F. Zipkin. 2025. Three decades of declines restructure butterfly communities in the Midwestern United States. Proceedings of the National Academy of Sciences 122:e2501340122.

581 Liebhold, A., W. D. Koenig, and O. N. Bjørnstad. 2004. Spatial Synchrony in Population
582 Dynamics*. Annual Review of Ecology, Evolution, and Systematics 35:467–490.
583 Liu, J., M. Vellend, Z. Wang, and M. Yu. 2018. High beta diversity among small islands is
584 due to environmental heterogeneity rather than ecological drift. Journal of
585 Biogeography 45:2252–2261.
586 Magurran, A. E., M. Dornelas, F. Moyes, and P. A. Henderson. 2019. Temporal β diversity—
587 A macroecological perspective. Global Ecology and Biogeography 28:1949–1960.
588 McCallum, M. L. 2015. Vertebrate biodiversity losses point to a sixth mass extinction.
589 Biodiversity and Conservation 24:2497–2519.
590 McCann, K. S., J. B. Rasmussen, and J. Umbanhowar. 2005. The dynamics of spatially
591 coupled food webs. Ecology Letters 8:513–523.
592 Melbourne, B. A., and A. Hastings. 2008. Extinction risk depends strongly on factors
593 contributing to stochasticity. Nature 454:100–103.
594 Nakadai, R. 2021. Individual-based multiple-unit dissimilarity: novel indices and null model
595 for assessing temporal variability in community composition. Oecologia 197:353–
596 364.
597 Olden, J. D., N. L. Poff, M. R. Douglas, M. E. Douglas, and K. D. Fausch. 2004. Ecological
598 and evolutionary consequences of biotic homogenization. Trends in Ecology &
599 Evolution 19:18–24.
600 Orrock, J. L., and J. I. Watling. 2010. Local community size mediates ecological drift and
601 competition in metacommunities. Proceedings of the Royal Society B: Biological
602 Sciences 277:2185–2191.
603 Otto, S. P., and M. C. Whitlock. 1997. The Probability of Fixation in Populations of
604 Changing Size. Genetics 146:723–733.

Pebesma, E. 2018. Simple Features for R: Standardized support for spatial vector data. The R Journal.

Pebesma, E., and R. Bivand. 2005. Classes and methods for spatial data in R. R News.

Pebesma, E., and R. Bivand. 2023. Spatial data science: with applications in R (1st ed.).

Pierce, D. 2023. ncdf4: Interface to Unidata netCDF (Version 4 or Earlier) Format Data Files_.

Ranta, E., V. Kaitala, J. Lindstr□m, and E. Helle. 1997. The Moran Effect and Synchrony in Population Dynamics. Oikos 78:136–142.

Reed, D. H., and G. R. Hobbs. 2004. The relationship between population size and temporal variability in population size. Animal Conservation 7:1–8.

Saito, V. S., N. E. Stoppa, E. M. Shimabukuro, M. Cañedo-Argüelles, N. Bonada, and T. Siqueira. 2021. Stochastic colonisation dynamics can be a major driver of temporal β diversity in Atlantic Forest coastal stream communities. Freshwater Biology 66:1560–1570.

Shimadzu, H., M. Dornelas, and A. E. Magurran. 2015. Measuring temporal turnover in ecological communities. Methods in Ecology and Evolution 6:1384–1394.

Siqueira, T., C. P. Hawkins, J. D. Olden, J. Tonkin, L. Comte, V. S. Saito, T. L. Anderson, G. P. Barbosa, N. Bonada, C. C. Bonecker, M. Cañedo-Argüelles, T. Datry, M. B. Flinn, P. Fortuño, G. A. Gerrish, P. Haase, M. J. Hill, J. M. Hood, K. Huttunen, M. J. Jeffries, T. Muotka, D. R. O'Donnell, R. Paavola, P. Paril, M. J. Paterson, C. J. Patrick, G. Perbiche-Neves, L. C. Rodrigues, S. C. Schneider, M. Straka, and A. Ruhi. 2024. Understanding temporal variability across trophic levels and spatial scales in freshwater ecosystems. Ecology 105:e4219.

628 Siqueira, T., V. S. Saito, L. M. Bini, A. S. Melo, D. K. Petsch, V. L. Landeiro, K. T. Tolonen,
629 J. Jyrkänkallio-Mikkola, J. Soininen, and J. Heino. 2020. Community size can affect
630 the signals of ecological drift and niche selection on biodiversity. Ecology 101.
631 Sokol, E., and T. Lamy. 2022. _ltmc: Long-term metacommunity analysis_.
632 Stefan, H. G., and E. B. Preud'homme. 1993. Stream Temperature Estimation from Air
633 Temperature1. JAWRA Journal of the American Water Resources Association 29:27–
634 45.
635 Steiner, C. F., R. D. Stockwell, V. Kalaimani, and Z. Aqel. 2013. Population synchrony and
636 stability in environmentally forced metacommunities. Oikos 122:1195–1206.
637 Suzuki, Y., and E. P. Economo. 2024. The stability of competitive metacommunities is
638 insensitive to dispersal connectivity in a fluctuating environment. The American
639 Naturalist.
640 Tatsumi, S., R. Iritani, and M. W. Cadotte. 2021. Temporal changes in spatial variation:
641 partitioning the extinction and colonisation components of beta diversity. Ecology
642 Letters 24:1063–1072.
643 Terui, A., and J. Pomeranz. 2023. _mcbrnet: Metacommunity simulation in branching
644 networks_.
645 Vellend, M. 2016. The Theory of Ecological Communities. Edição: Mpb Series: 57 ed.
646 Princeton University Press, Princeton.
647 Vindenes, Y., and S. Engen. 2017. Demographic stochasticity and temporal autocorrelation in
648 the dynamics of structured populations.
649 https://onlinelibrary.wiley.com/doi/abs/10.1111/oik.03958.
650 Wang, S., T. Lamy, L. M. Hallett, and M. Loreau. 2019. Supp material: Stability and
651 synchrony across ecological hierarchies in heterogeneous metacommunities: linking
652 theory to data. Ecography 42:1200–1211.

Whitlock, M. C. 2004. Selection and Drift in Metapopulations. Pages 153–173 Ecology, Genetics and Evolution of Metapopulations. Elsevier.

Wickham, H., M. Averick, J. Bryan, W. Chang, L. McGowan, R. François, G. Grolemund, A. Hayes, L. Henry, J. Hester, M. Kuhn, T. Pedersen, E. Miller, S. Bache, K. Müller, J. Ooms, D. Robinson, D. Seidel, V. Spinu, K. Takahashi, D. Vaughan, C. Wilke, K. Woo, and H. Yutani. 2019. Welcome to the tidyverse. Journal of Open Source Software.

Willi, Y., J. van Buskirk, and A. A. Hoffmann. 2006. Limits to the Adaptive Potential of Small Populations. Annual Review of Ecology, Evolution, and Systematics 37:433–458.

Xiao, J., Y. Feng, H. Zhang, C. Xu, K. Zhang, M. W. Cadotte, and L. Cheng. 2025. The proportion of low abundance species is a key predictor of plant β-diversity across the latitudinal gradient. Journal of Ecology 113:795–805.

668 **Table 1.** Summary of fixed effects from the Gaussian location-scale GLMM modeling
669 temporal β-diversity (rank change). The model includes ecological predictors related to local
670 community size, environmental variability, and species richness. PL = proportion of species
671 in the lowest abundance category. All predictors were standardized prior to model fitting. All
672 Wald chi-square tests were performed with 1 degree of freedom.
673

Predictor	**Estimate**	**Std. Error**	**Wald χ^2**	**p-value**
Conditional Model (Mean)				
(Intercept)	0.152	0.006	–	2e-16
Community size	–0.006	0.002	9.29	0.0023
CV of community size	0.013	0.002	28.95	7.44e-08
PL	0.004	0.003	2.28	0.1315
CV of min. temperature	0.007	0.006	1.81	0.1785
CV of max. temperature	–0.000	0.005	0.000	0.9965
CV of precipitation	0.007	0.004	3.24	0.0717
Species richness	0.017	0.003	26.96	2.08e-07

674
675

Table 2. Summary of fixed effects from the beta regression used to model temporal variability in spatial β-diversity. The model includes ecological predictors related to community size, environmental variability, and species richness. PL = proportion of species in the lowest abundance category. All predictors were standardized prior to model fitting. All Wald chi-square tests were performed with 1 degree of freedom.

Predictor	**Estimate**	**Std. Error**	**Wald χ^2**	***p*-value**
Intercept	–2.468	0.072	–	2e-16
Metacommunity size	–0.032	0.091	0.12	0.7250
Median PL	0.010	0.108	0.01	0.9278
CV of PL	0.183	0.113	2.61	0.1059
Spatial extent	0.041	0.070	0.34	0.5620
Synchrony precipitation	–0.153	0.073	4.42	0.0356
CV of metacommunity size	0.138	0.076	3.29	0.0699
Gamma diversity	0.028	0.111	0.06	0.8020

685

686 **Figure 1.** Partial effects of main predictors ($p < 0.05$) on predicted temporal variability in
687 species composition (rank change) from the best-fitting Gaussian GLMM. (a) Local
688 community size, (b) coefficient of variation of community size, and (c) estimated species
689 richness. Shaded areas represent 95% confidence intervals. All predictors were scaled (mean
690 = 0, SD = 1) prior to model fitting.

691

692

693

694

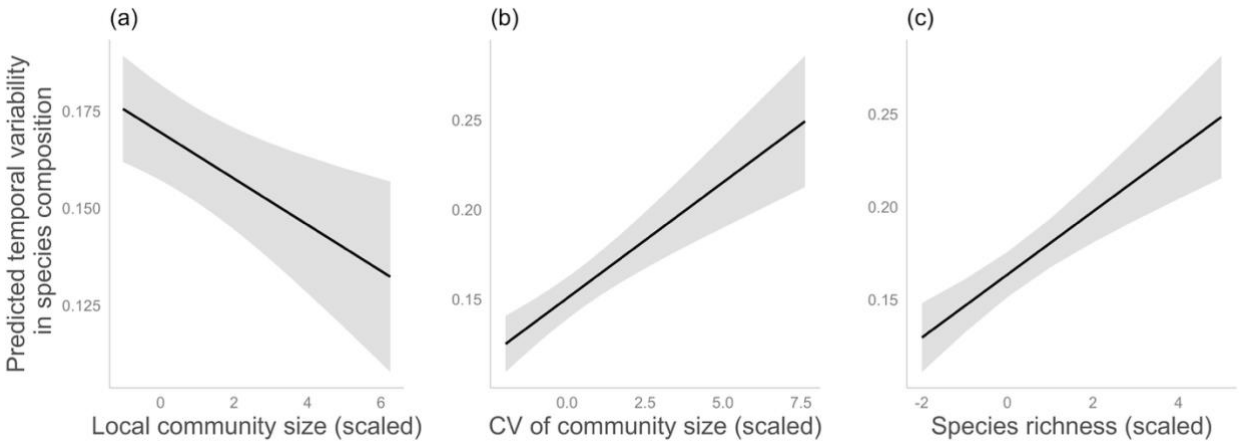

695

696 Figure 1.

697

698 **Appendix S1.**

699 **Table S1.** Model selection for the analysis of temporal variability. Top: Local-scale analysis
700 of temporal β-diversity (rank change). Bottom: Regional-scale analysis of temporal
701 variability in spatial β-diversity (CV_rank). Abbreviations: df: degrees of freedom; AIC:
702 Akaike Information Criterion; ΔAIC: difference in AIC relative to the best model in each
703 section; BIC: Bayesian Information Criterion; logLik: log-likelihood; LRT: Likelihood-ratio
704 test.

Model	Description	df	AIC	ΔAIC	logLik	LRT χ^2	χ^2 df	Pr(>χ^2)
Local-Scale Models								
fit1	Fixed effects only (Gaussian)	9	-1225.2	151.2	621.61	-	-	-
fit2	+ Random intercept	10	-1318.5	58.0	669.25	95.28	1	< 2e-16
fit3	+ Dispersion submodel (Full Gaussian)	13	-1376.4	0.0	701.21	63.93	3	8.5e-14
fit_beta	Beta distribution (Full structure)	13	-1376.4	0.0	701.21	-	-	-
fit_gauss	Gaussian distribution (Full structure)	13	-1299.9	76.5	662.96	0	0	1
Regional-Scale Models								
fit1.r	Fixed effects only (Beta)	9	-144.65	0.1	81.33	-	-	-
fit2.r	+ Dispersion submodel (Beta)	13	-144.59	0.0	85.29	7.94	4	0.094
fit_beta.r	Beta distribution (Selected)	9	-144.65	0.0	81.33	-	-	-
fit_gauss.r	Gaussian distribution	9	-134.45	10.2	76.22	0	0	1

705

706

707

Table S2. Statistics obtained in the process-based simulation model by relating the metrics of temporal variability in species composition with the median community size. Simulations were conducted using different seeds and dispersal rates. The p-value represents the significance of each relationship, and the explanatory power was measured by R^2.

Temporal variability metric	set.seed	Dispersal	Slope	p-value	R^2	Adjusted R^2
LTMC local	1234	0.1	-1.2E-04	0.0055	0.1901	0.1683
LTMC regional	1234	0.1	-6.4E-06	0.0985	0.0721	0.0470
Rank change	1234	0.1	1.0E-06	0.8411	6.3E-05	-0.0015
Rank difference	1234	0.1	1.1E-05	0.0017	0.0252	0.0227
LTMC local	1234	0.5	-3.8E-05	0.0132	0.1549	0.1321
LTMC regional	1234	0.5	-1.2E-06	0.6211	0.0067	-0.0202
Rank change	1234	0.5	8.6E-06	0.0364	0.0069	0.0053
Rank difference	1234	0.5	4.2E-06	0.301	0.0028	0.0002
LTMC local	1234	1	-3.7E-05	0.0108	0.1632	0.1406
LTMC regional	1234	1	-2.3E-06	0.405	0.0188	-0.0077
Rank change	1234	1	5.0E-07	0.9071	2.2E-05	-0.0016
Rank difference	1234	1	1.2E-05	0.0091	0.0174	0.0149
LTMC local	111	0.1	-1.3E-04	0.0001	0.328	0.3098
LTMC regional	111	0.1	-9.0E-06	0.0021	0.2274	0.2065
Rank change	111	0.1	-2.3E-07	0.9565	4.8E-06	-0.0016
Rank difference	111	0.1	1.4E-05	1.5E-06	0.0580	0.0556
LTMC local	111	0.5	-4.6E-05	0.0003	0.3016	0.2827
LTMC regional	111	0.5	-6.7E-06	0.0060	0.1868	0.1648
Rank change	111	0.5	6.3E-06	0.1187	0.0039	0.0023
Rank difference	111	0.5	2.1E-05	2.1E-08	0.0778	0.0754
LTMC local	111	1	-4.3E-05	0.0003	0.3063	0.2875
LTMC regional	111	1	-5.5E-06	0.0255	0.1278	0.1042
Rank change	111	1	-4.8E-07	0.9029	2.4E-05	-0.0016
Rank difference	111	1	1.7E-05	1.4E-05	0.0476	0.0451

Table S3. Summary of fixed effects from the dispersion component of the Gaussian GLMM, where the log of the residual variance was modeled as a linear function of ecological predictors (i.e. log-linear dispersion model). This structure accounts for heteroscedasticity in the response variable by allowing residual variance to vary across observations as a function of median community size, the coefficient of variation (CV) in community size, and the proportion of species in the lowest abundance category (PL). The table reports estimated effects, standard errors, and z-values from Wald z-tests. All predictors were standardized prior to model fitting.

Predictor	**Estimate**	**Std. Error**	**z value**	***p*-value**
(Intercept)	–2.902	0.035	–82.460	2e-16
Median local community size	–0.333	0.040	–8.270	2e-16
CV of local community size	–0.115	0.035	–3.250	0.00117
PL	–0.167	0.032	–5.290	1.19e-07

Supplementary Figures

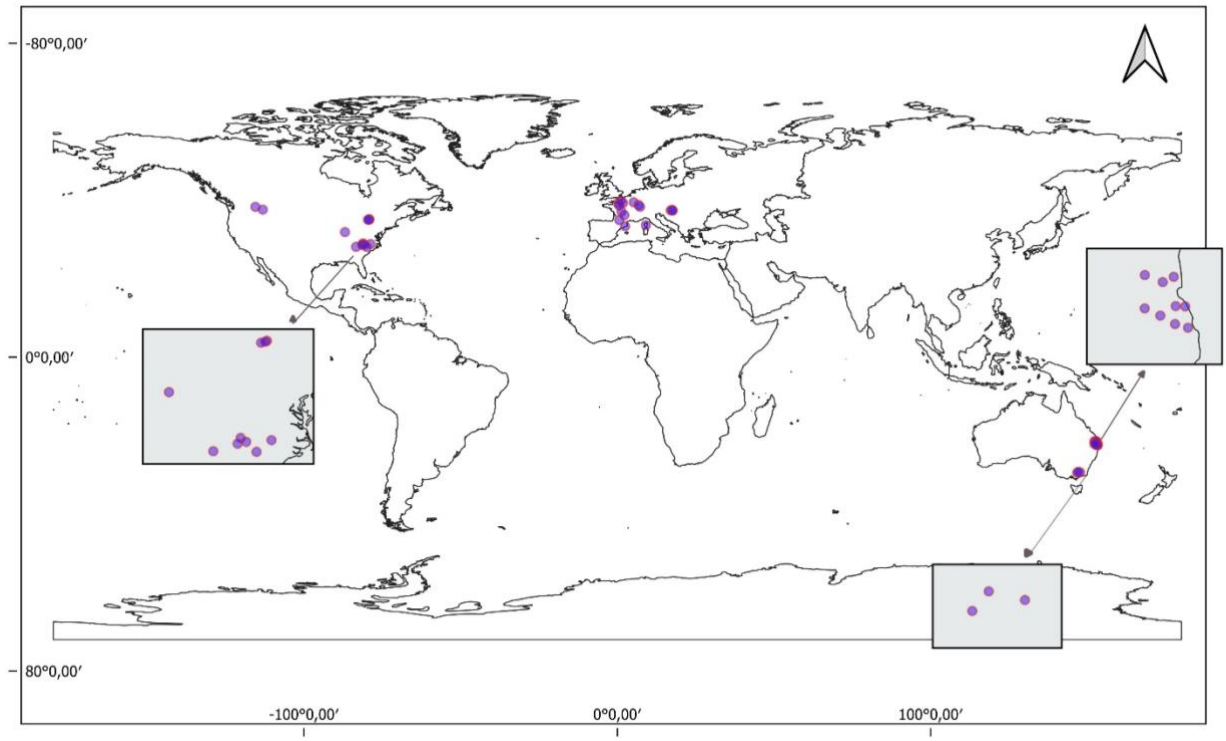

Figure S1. Geographic distribution of the 39 metacommunities selected in our study, located in Australasia (12), Nearctic (12), and Palearctic (15) biogeographical realms.

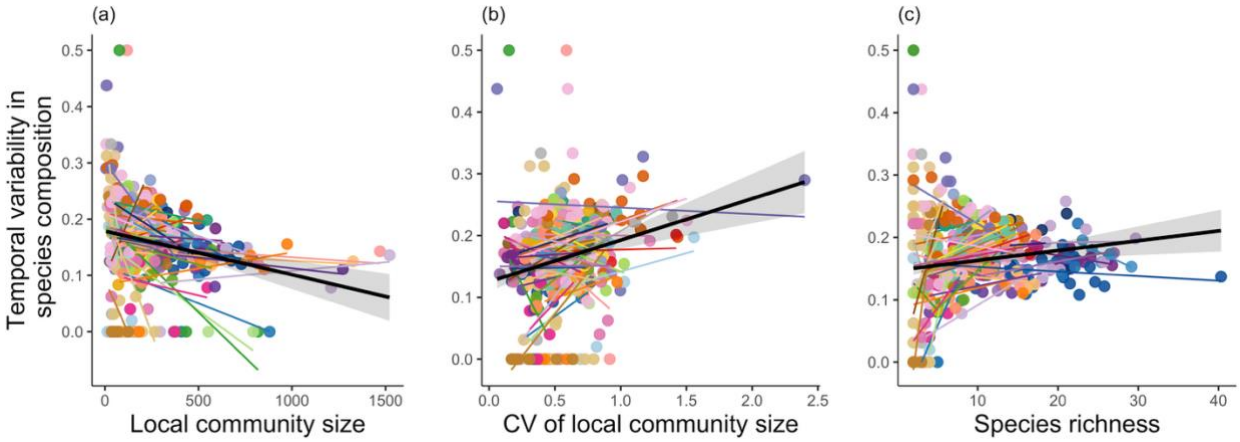

Figure S2. Raw data on temporal variability in species composition (rank change) plotted against (a) local median community size, (b) coefficient of variation (CV) of local community size, and (c) estimated species richness for individual metacommunities (colors). Colored lines are exploratory visual aids (e.g., local trends), not model components. The black thicker line represents the overall relationship, with the grey band representing a 95% confidence interval.